



DOI: 10.5281/zenodo.3960201

## EVALUATION OF NANOLIME DISPERSIONS FOR THE PROTECTION OF ARCHAEOLOGICAL CLAY-BASED BUILDING MATERIALS

Anastasia Michalopoulou<sup>\*1,2</sup>, Noni-Pagona Maravelaki<sup>2</sup>, Nikolaos-Alexios Stefanis<sup>3</sup>, Panagiotis Theoulakis<sup>3</sup>, Stelios Andreou<sup>4</sup>, Vassilis Kilikoglou<sup>1</sup> and Ioannis Karatasios<sup>1</sup>

<sup>1</sup>*Institute of Nanoscience and Nanotechnology, National Centre for Scientific Research "Demokritos",  
Agia Paraskevi, 153 10 Athens, Greece*

<sup>2</sup>*School of Architecture, Technical University of Crete, Akrotiri, 73100 Chania, Greece*

<sup>3</sup>*Department of Conservation of Antiquities and Works of Art,  
University of West Attica, Egaleo Park, 122 43 Athens, Greece*

<sup>4</sup>*Department of Archaeology, Aristotle University of Thessaloniki, 54124 Thessaloniki, Greece*

Received: 29/06/2020

Accepted: 28/08/2020

\*Corresponding author: a.michalopoulou@inn.demokritos.gr

### ABSTRACT

Clay-based building materials have been very popular in construction and common in cultural heritage sites around the Mediterranean. The excavation of the Late Bronze Age settlement of Thessaloniki Toumba (northern Greece), revealed an abundance of this type of material with apparent preservation problems mainly caused by swelling phenomena due to water absorption and/or humidity fluctuations. This led to the alteration of the structural and aesthetic integrity of the archaeological findings, jeopardizing the preservation of the site and as a consequence, the archaeological evidence that they contain. Triggered by the identification of swelling clay phases in the sixteen samples of mud-bricks, this work studies the effectiveness, in terms of anti-swelling action, of two different categories of calcium hydroxide materials: saturated solution of calcium hydroxide (limewater) and various types of laboratory produced nano-lime dispersions. The effect of the dispersion medium (water and mixed polar solvents) on the reactivity of calcium hydroxide with clays and the stabilization of their microstructure were investigated on laboratory produced clay briquettes containing different percentages of montmorillonite (1, 5 and 15 % w/w).

The interpretation of mineralogical (XRD) and chemical results (FTIR) highlighted the significance of the dispersion medium for the treatments and the beneficial role of laboratory prepared nano-lime dispersions when they are used as swelling inhibitors. Nanolimes were able to react and stabilize the external layers of clays through the formation of C-S-H, thus resulting in increased durability of mud- briquettes against swelling.

---

**KEYWORDS:** Bronze Age Tumba, Nanolime, Mud bricks, Adobe structures, Swelling clays, Montmorillonite, Consolidation, Earthen Architecture, Conservation

---

## 1. INTRODUCTION

Clay (or mud) has been widely used, since the prehistoric times for building (Minke 2012). Clay-based building materials can be classified in many categories in terms of the preparation process and use, such as mud-bricks, clay-plasters, cob and rammed earth (Garcia-Vera *et al.*, 2018; Lawrence *et al.*, 2009; Emiroğlu *et al.*, 2015). They are frequently found in many archaeological and cultural heritage sites of the Mediterranean basin, shaping the field of earthen architecture (El-Derby *et al.*, 2016; El-Gohary *et al.*, 2009; Jimenez-Delgado *et al.*, 2006; Lanzon *et al.*, 2020; Quagliarini *et al.*, 2010). The majority of earthen architecture monuments consisted of hand-made mud-bricks produced by a mixture of earth and water, which was then left to dry under natural environmental conditions (Quagliarini *et al.*, 2015). Mud-bricks are, therefore, composite building materials consisting of a variety of non-plastic components (such as rock fragments and organic fibres) and clay minerals, which act as binder (Elert *et al.*, 2015; Hall *et al.*, 2004). The extensive diachronic use of this type of building materials is related to their wide availability (soil and water) and low cost (Garcia-Vera *et al.*, 2018).

However, clay-based building materials present limited durability against water-related degradation processes, such as capillary absorption, wetting-drying cycles, freeze-thaw and soluble salt crystallization (Rainer, 2008; Chen *et al.*, 2018; Crosby, 1988). Moreover, the deleterious role of water is associated with the swelling phenomenon of clay minerals and the subsequent effect on the degradation of the structure.

The prehistoric settlement of Thessaloniki Toumba in northern Greece, is an example of extensive use of mud-bricks for building and it offers a unique opportunity to expand our knowledge on the technology and conservation of such materials. The settlement is located in the Ano Toumba district on the low hills of the north-east part of Thessaloniki, 1.7 km from the present coast of Thermaikos bay and at an altitude of 73 m. The excavations indicate that the site was occupied between 2000 B.C. and the end of the 4<sup>th</sup> century B.C. The mud-brick material included in this study were excavated at the summit of the mound, where the houses of the LBA phase of the settlement were located, tightly clustered (Andreou, 2007; Andreou *et al.*, 1996). The primary building material used for the construction was mud-bricks reinforced with wooden posts (Andreou *et al.*, 1996). It is worth noting that the LBA settlement has not faced fire or any similar destruction and, therefore, mud-bricks have not undergone any heating process (Andreou, 2007).

The technological study of mud bricks through mineralogy and chemistry is of particular interest since this type of material usually does not survive for long periods and unburned findings from the Bronze Age are rare. Moreover, the study of the correlation between technological choices, material properties, and performance contribute to the study of technology evolution through time at different societal contexts (Lorenzon *et al.*, 2020; Love, 2012; Xanthopoulou *et al.*, 2020).

The role of water in the study of the preservation of archaeological mud-bricks is very essential since it is responsible for the swelling of expansive clay minerals, leading to disordering and collapse (Stefanis *et al.*, 2010). The swelling phenomenon is connected with the presence of smectite group clays or commonly known as swelling clays (Salles *et al.*, 2013). The event of swelling occurs when polar molecules like water are adsorbed and enter in the inter-planar plane and cause the expansion of the inter-layer, and thus the development of internal stresses and the eventual failure of the material (Hensen and Smit, 2002; Pham *et al.*, 2014; Shalles *et al.*, 2013; Stefanis *et al.*, 2010; Wangler *et al.*, 2008).

The severe damage-risk of the mud-bricks underlines the need for protection through consolidation for the re-establishment of the mud-bricks' coherence and stabilization of the swelling-clays structure for preventing further degradation of the archaeological material.

Regarding the preservation of clay-based materials, in addition to the necessary cleaning treatments of the excavated material (Abd-Allah *et al.*, 2010; Saenz-Martinez *et al.*, 2020), the main concern is their physicochemical stabilization. In general, the stabilization of earthen materials can be implemented through three paths: mechanical, physical and chemical (Medjo Eko *et al.*, 2012; Quagliarini *et al.*, 2015). Mechanical stabilization concerns the increase of the density of soil by compaction and thus increasing the mechanical strength. Physical stabilization involves the exploitation of properties like firing, electro-osmosis or soil structure improvement (Menjo Eko *et al.*, 2012; Maskell *et al.*, 2014; Quagliarini *et al.*, 2015). Finally, chemical stabilization involves the use of additives or stabilizers as a means to modify the chemical characteristics of the clay-based material and thus reduce the hydrometric shrinkage.

The combination of consolidation with stabilization re-establishes the internal cohesion of the loose layers and inhibits the hydrometric shrinkage enabling them to maintain the valuable archaeological and contextual information (Garcia-Vera *et al.*, 2020; Karatasios *et al.*, 2009; Maravelaki-Kalaitzaki *et al.*, 2008; Michalopoulou *et al.*, 2020). To this direction, a

promising consolidation agent with swelling-inhibition properties of smectite minerals (Lanzon et al., 2020) is the group of alkaline activators such as saturated calcium hydroxide solutions (limewater) and  $\text{Ca}(\text{OH})_2$  nano-dispersions (nanolime) (Elert, et al., 2015; Garcia-Vera et al., 2020). These materials have already been tested during the laboratory consolidation research for the conservation and preservation of famous monuments like the Great Wall of the Ming Dynasty in China (Chen et al., 2018), the soil and the earthen wall in the Generalife garden in the Alhambra palace in Spain (Elert et al., 2015; Lanzon et al., 2020) and the Aztec-Period Rural Sites in Mexico (Camerini et al., 2018).

The effective role of  $\text{Ca}(\text{OH})_2$  is based on the short term and long term interactions with clay-phases, in the presence of water (Ouhandi et al., 2014). In short-term, cation exchange is implemented in the presence of  $\text{CaO}$  in soils, causing the reduction of the repulsion forces between the alumino-silicate layers and the eventual flocculation of layers, thus improving them concerning the swelling and shrinkage properties (Ouhandi et al., 2014; Seco et al., 2011). In the long-term, under alkali environmental conditions (with the excess of  $\text{OH}^-$ ), silica and alumina dissolve from the alumino-silicate layers and react with the  $\text{Ca}^{2+}$  through the realization of the pozzolanic reaction (Daniele et al., 2013) and form cementitious compounds such as calcium silicate hydrates (CSH), calcium aluminate hydrates (CAH) and calcium alumino-silicate hydrates (CASH) (Elert et al., 2015; Ouhandi et al., 2014; Seco et al., 2011; Zarzuela et al., 2020).

Compared to the traditional calcium hydroxide saturated water solutions, nanolime dispersions are characterized by a higher concentration of the active component, presenting a way to overcome the need of high repeatability of the saturated water solutions due to the low solubility of  $\text{Ca}(\text{OH})_2$  in water (Garcia-Vera et al., 2020). The size and shape of the  $\text{Ca}(\text{OH})_2$  nanoparticles, along with the selection of the appropriate dispersion media have a critical im-

act on the efficiency of the consolidation action since they affect the penetration ability of the dispersions and the surface area of the  $\text{Ca}(\text{OH})_2$  nanoparticles, and thus their reactivity (Borsoi et al., 2016; Michalopoulou et al., 2018; 2020; Otero et al., 2020; Salama et al., 2020).

This paper studies the material properties of clays used for the production of mud-bricks found in the prehistoric settlement of Thessaloniki Toumba in northern Greece and how these affect their durability and preservation of the archaeological site. For this reason, mineralogical and chemical characterisation of the sixteen clay samples was carried out as well as their durability when subjected to artificial weathering of wet/drying cycles was measured.

Based on the physicochemical data, the potential anti-swelling role and protective effect of different forms of calcium hydroxide were studied. Calcium hydroxide was used in two forms: saturated solution of calcium hydroxide (traditional limewater) and various types of laboratory composed nanophase lime. The preservation mechanism was studied using laboratory replicas (briquettes) simulating the original material and containing different percentages of montmorillonite (1, 5 and 15 %wt).

Aiming to contribute to the field of conservation of mud-bricks, emphasis was given on the stabilization of clay microstructure, by investigating the in-situ interaction between calcium hydroxide and clay-phases, depending on the dispersion medium of the consolidation agent (water and mixed polar dispersion medium).




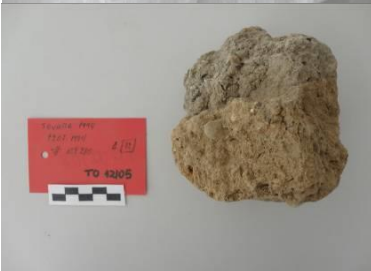


## 2. MATERIALS AND METHODS

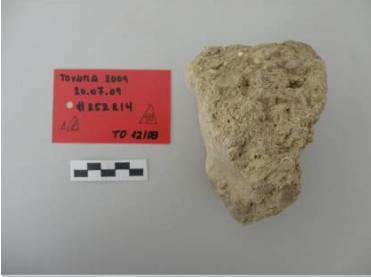

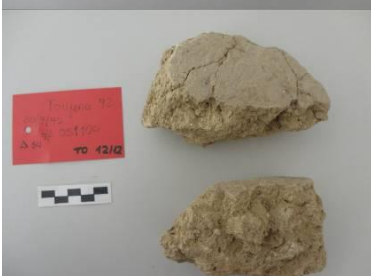

### 2.1. Archaeological samples

Sixteen representative mud-brick samples coming from LBA structures were collected. All sixteen samples were macroscopically characterized as unfired clay with the compact structure containing, imprints and straw traces used for the reinforcement of the matrix (Table 1).

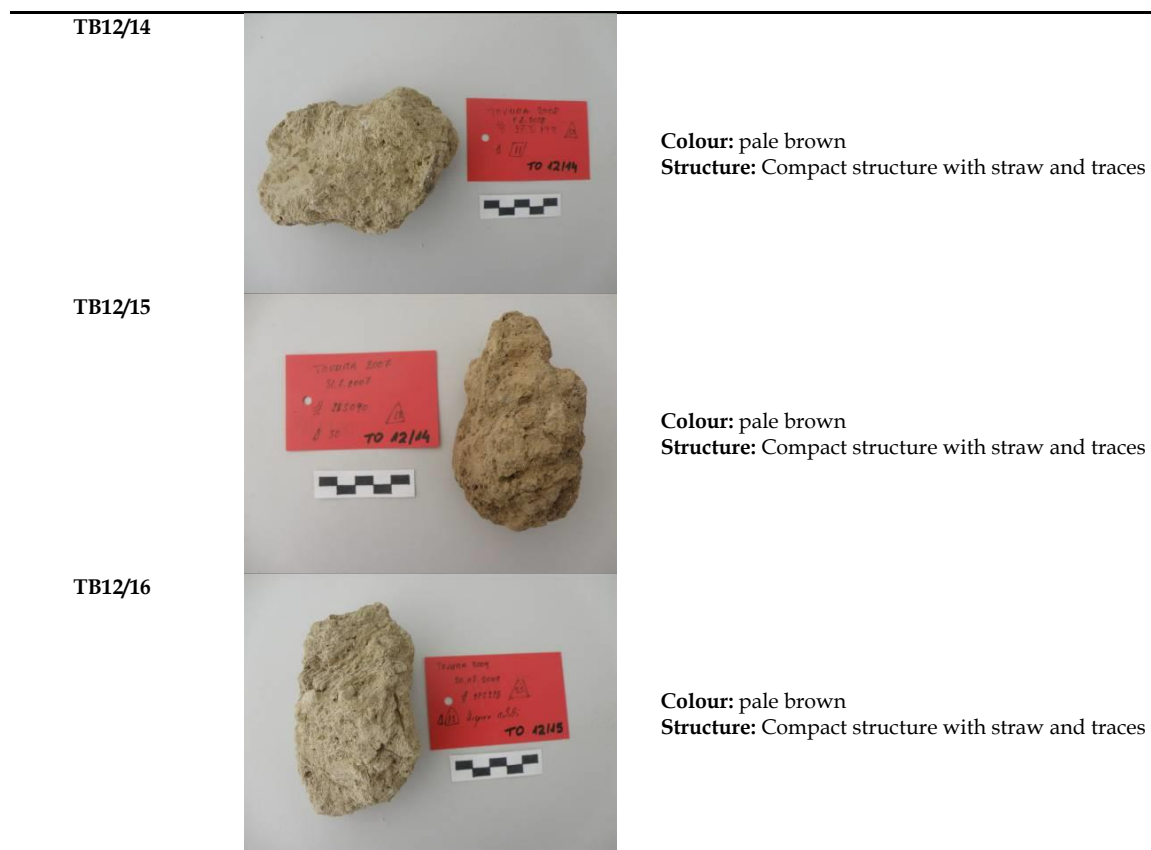
*Table 1 Macroscopic description of the 16 mud-brick samples from the prehistoric settlement of Thessaloniki Toumba, Greece*

Samples I.D.		Description
TB12/01		<p><b>Colour:</b> reddish brown  <b>Structure:</b> Compact structure with straw traces</p>

TB12/02		<p><b>Colour:</b> red  <b>Structure:</b> Compact structure with straw traces</p>
TB12/03		<p><b>Colour:</b> reddish yellow  <b>Structure:</b> Compact structure with straw traces</p>
TB12/04		<p><b>Colour:</b> red  <b>Structure:</b> Compact structure with charcoal and straw traces</p>
TB12/05		<p><b>Colour:</b> reddish brown  <b>Structure:</b> Compact structure with straw traces</p>
TB12/06		<p><b>Colour:</b> reddish brown  <b>Structure:</b> Compact structure with straw and traces</p>
TB12/07		<p><b>Colour:</b> reddish brown  <b>Structure:</b> Structure characterized by the presence of cracks and straw traces</p>

TB12/08		<p><b>Colour:</b> pale brown  <b>Structure:</b> Compact structure with straw and traces</p>
TB12/09		<p><b>Colour:</b> pale brown  <b>Structure:</b> Compact structure with straw and traces</p>
TB12/10		<p><b>Colour:</b> pale brown  <b>Structure:</b> Compact structure with straw and traces</p>
TB12/11		<p><b>Colour:</b> pale brown  <b>Structure:</b> Compact structure with straw and traces</p>
TB12/12		<p><b>Colour:</b> pale brown  <b>Structure:</b> Compact structure with straw and traces</p>
TB12/13		<p><b>Colour:</b> pale brown  <b>Structure:</b> Compact structure with straw and traces</p>





## 2.2. Mineralogical and Chemical Characterization of Mud-bricks

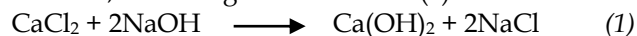
The characterization of mud-bricks was carried out by x-ray diffraction analysis (XRD) and energy dispersive X-ray spectroscopy (EDS). A representative amount of about 100 g from each sample was received after physical/mechanical separation without affecting the integrity of the aggregate inclusions (rock fragments). The material with grain size below 63  $\mu\text{m}$  was used for the characterization of the clay fraction. The mineralogical analysis was carried out on treated samples with a dilute solution of acetic acid (5 % wt). The chemical treatment was implemented for the removal of the calcareous phases, to facilitate the detection and identification of the clay minerals. The acid treatment involved the mixing of 5 g of the archaeological material (<125  $\mu\text{m}$ ) with a 100 ml of dilute acid solution, under magnetic stirring. Then the liquid excess was removed and replaced with fresh dilute acid solution. The process was repeated several times upon the absence of any bubbling phenomenon. The solid residue was then collected, rinsed with deionized water and then left upon drying in the oven ( $T < 100^\circ\text{C}$ ). Finally, the treated materials were subjected to grinding for the preparation of the samples.

## 2.3. Artificial ageing test- wet/drying cycles

Twelve out of the sixteen samples were selected and placed separately on filtration papers in packed beds. In every cycle, the packed bed was soaked with deionized water that was absorbed from the mud-bricks through capillary. The water saturation of the mud-bricks was implemented quickly. Then the mud-bricks were left to dry to enable the macroscopic effect of the wet/drying cycle. The procedure was repeated two times since the shape of the samples was affected and disordered.

## 2.4. Preparations of $\text{Ca}(\text{OH})_2$ based consolidants

Three calcium hydroxide ( $\text{Ca}(\text{OH})_2$ ) treatments were prepared for studying their reactivity with clays and their consolidation/stabilization ability (Table 2). The first two treatments (NW and N/w+isp) were laboratory composed colloidal dispersions of  $\text{Ca}(\text{OH})_2$ , via the bottom-up process. The bottom-up process concerns the displacement reaction between calcium chloride  $\text{CaCl}_2$  (0.3 mol/L) and sodium hydroxide NaOH (0.6 mol/L) in an aqueous solution, according to the reaction (1):



The sodium hydroxide aqueous solution ( $\text{NaOH} \geq 98\%$ , Sigma-Aldrich) was added drop by drop in the calcium chloride aqueous solution ( $\text{CaCl}_2 \cdot \text{H}_2\text{O} \geq 99\%$ , Sigma-Aldrich) in an inert atmosphere (He) to

avoid the rapid initiation of the carbonation of the newly synthesized  $\text{Ca}(\text{OH})_2$  nanoparticles (Lanzon et al., 2017; Michalopoulou et al., 2020). The final products were calcium hydroxide nanoparticles  $\text{Ca}(\text{OH})_2$  and the water soluble sodium chloride  $\text{NaCl}$ , which was removed by continuous washings with distilled water. The implementation of the bottom-up process led to the production of aqueous nanolime dispersions of concentration of 1,1% w/v (**NW**). To study the effect of the modification of the dispersion medium, in a second dispersion, the distilled water was replaced with a mixed polar dispersion medium

(**N/w+isp**) (Daniele et al., 2012; Michalopoulou et al., 2018;2020). The dispersions (Table 2) were then placed for ultrasonic agitation (UIP 1000 hdT Hielsner), for disaggregation of any agglomerates derived from the synthetic procedure.

Similar to the procedure described in the literature (Rodriguez-Navarro et al., 2013), a saturated aqueous  $\text{Ca}(\text{OH})_2$  solution was produced via the dissolution of laboratory produced lime putty ( $d=1.75 \text{ g/cm}^3$ ) in distilled water, under continuous stirring (**LW**).

Table 1  $\text{Ca}(\text{OH})_2$  consolidation treatments

I.D.	Sample	Active component	Dispersion medium	
NW	Colloidal Dispersion	$\text{Ca}(\text{OH})_2$	Water 100%	2-propanol -
N/w+isp	Colloidal Dispersion	$\text{Ca}(\text{OH})_2$	10%	90%
LW	Saturated Solution	$\text{Ca}(\text{OH})_2$	100%	-

Mineralogical characterization of the samples was implemented by X-ray diffraction (XRD), in a Siemens D-500 diffractometer, using the  $\text{Cu-K}\alpha$  radiation ( $\lambda = 1.5406 \text{ \AA}$ ). The diffractograms were collected in the range of  $5-55^\circ 2\theta$  scale, with a step of  $0.03^\circ/3\text{sec}$ . All liquid samples were deposited on Si-wafers adjusted on typical XRD holders and left to dry under laboratory conditions.

Chemical characterization was implemented by Fourier-transform infrared spectroscopy (FTIR). A drop of the liquid samples was placed on a Si-wafer, left upon drying and then stored in the oven for 3 days at approximately  $80^\circ\text{C}$ . Spectra were collected on transmission mode, in the range of  $4000$  to  $400 \text{ cm}^{-1}$  (resolution  $4 \text{ cm}^{-1}$ ), with the use of a Bruker-Tensor 27 spectrometer.

The morphological characterization was implemented by Scanning Electron Microscope coupled with Energy Dispersive X-ray analyzer (SEM/EDX). SEM images were acquired in a FEI Quanta Inspect instrument operated at  $25 \text{ kV}$ . All samples were de-

posited on SEM-holders and were gold-coated prior to examination.

The X-ray diffractograms of all three  $\text{Ca}(\text{OH})_2$  consolidation treatments indicated the formation of portlandite with hexagonal crystal structure (Fig. 1). Minor phase of calcite ( $\text{CaCO}_3$ ) particles were also identified. The presence of calcite was related with the rapid initiation of the carbonation reaction (Michalopoulou et al., 2020).

SEM images (Fig. 2) present the clusters of  $\text{Ca}(\text{OH})_2$  nanoparticles formed during the drying of the samples on the stub. The aqueous nanolime dispersion **NW** resulted in plate like  $\text{Ca}(\text{OH})_2$  nanoparticles, characterized by dimensions between  $150$  and  $450 \text{ nm}$  and by uniform size (Fig. 2a). The hydroalcoholic nanolime dispersion **N/w+isp** resulted in hexagonal, spherical and of undetermined shape  $\text{Ca}(\text{OH})_2$  nanoparticles of dimensions between  $200$  to  $800 \text{ nm}$  (Fig. 2b). The saturated aqueous lime solution **LW** resulted in the formation of large angular  $\text{Ca}(\text{OH})_2$  particles of polydispersity in terms of size (Fig. 2c).

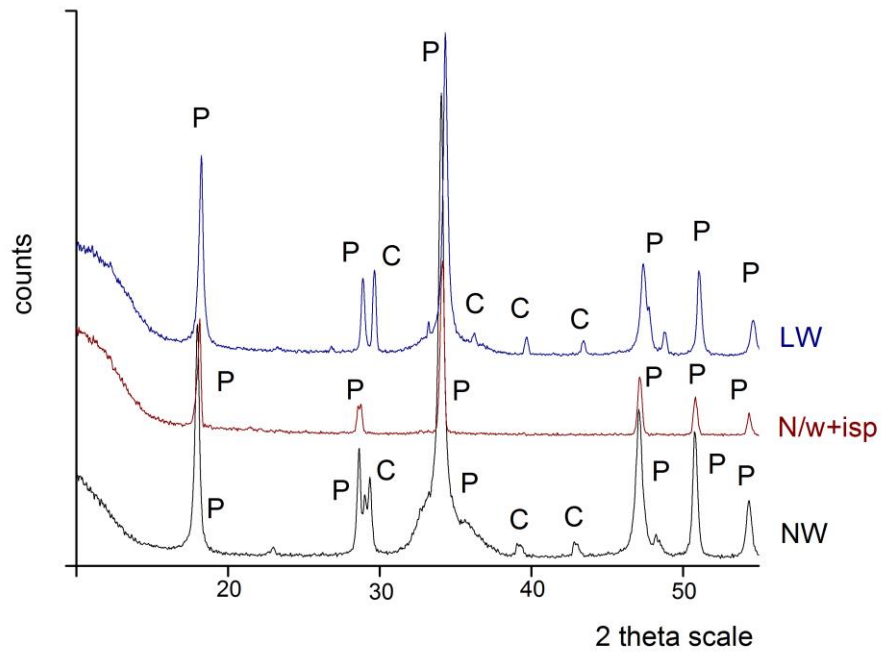


Fig. 1 X-ray diffraction pattern of the three  $\text{Ca}(\text{OH})_2$  treatments

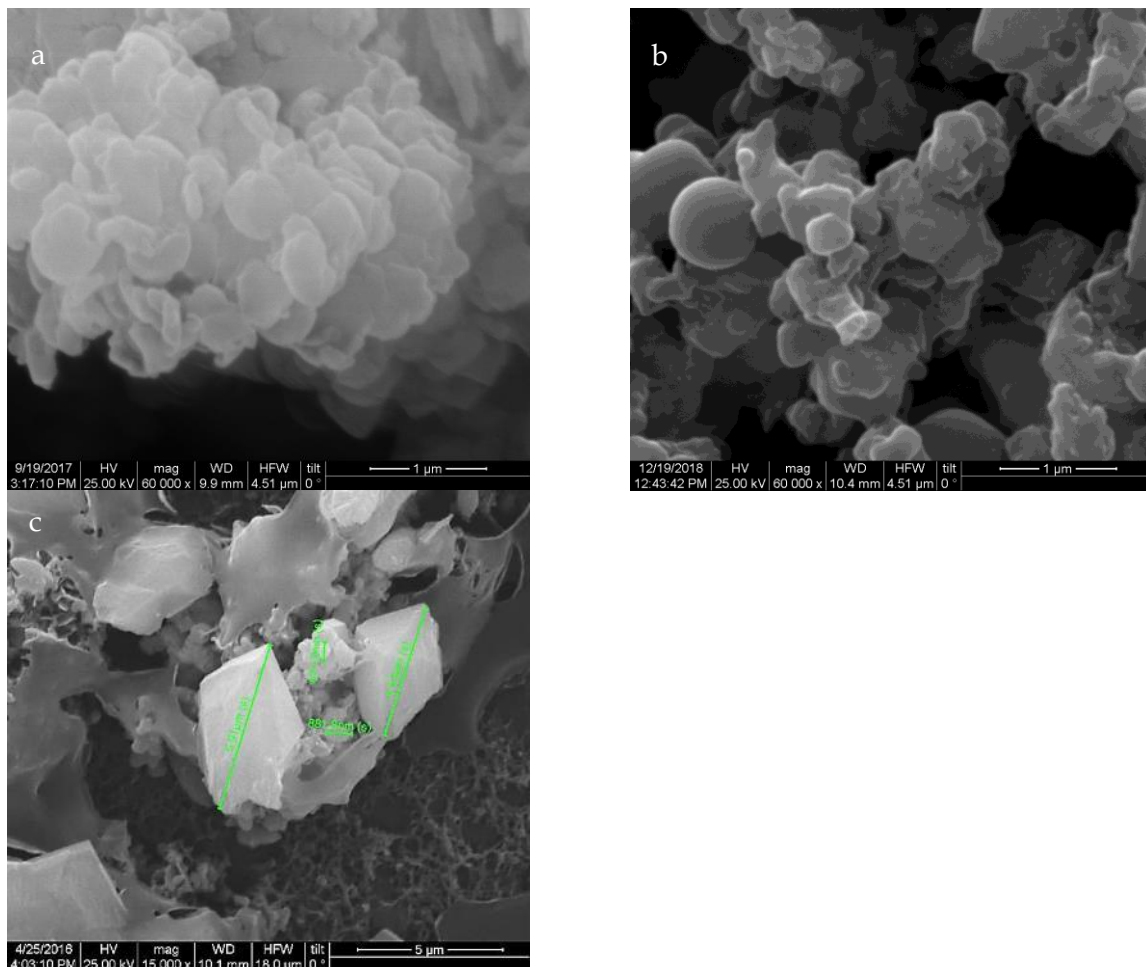


Fig. 2 SEM observation of the morphological characteristics of the  $\text{Ca}(\text{OH})_2$  consolidation treatments a) NW; b) N/w+isp and c) LW



## 2.5. Preparation of artificial clay samples for studying the consolidation effectiveness

The consolidation action of  $\text{Ca}(\text{OH})_2$  treatments was carried out in two different modules.

The first module concerned the investigation of the possible in-situ interaction between the  $\text{Ca}(\text{OH})_2$  and clays, to inhibit the swelling action of montmorillonite. Clay powder enriched with 1%wt of montmorillonite was mixed with the two nanolime dispersions and the saturated  $\text{Ca}(\text{OH})_2$  solution at 1:1 ratio (Table 3). The treated clay mixtures were characterized in terms of morphological characteristics after 24 hours and 1 month and in terms of the mineralogical and chemical composition of their reaction products, for 2 months.

Table 2 pH of the  $\text{Ca}(\text{OH})_2$  treatments before mixing with montmorillonite enriched clay specimens

Sample	pH
$\text{Ca}(\text{OH})_2$	Montmorillonite content of clay specimens (% wt)
NW	1
N/w+isp	1
LW	1
	12.3
	12.2
	12.4

The second module concerned the study of the potential modification of the swelling properties, and thus the microstructural and physical properties of laboratory synthesized clay briquettes of different swelling capacities. Three dry mixtures were synthesized, adding three different percentages of montmorillonite (1, 5 and 15 % w/w), along with a montmorillonite-free reference mixture. After the addition of water, rectangular prismatic specimens were formed and left to dry until constant weight, at  $60 \pm 5$  °C. The three  $\text{Ca}(\text{OH})_2$  treatments were applied drop to drop on the top face of the rectangular prismatic specimens, using a pipette (Fig. 3). The consolidation procedure was repeated ten times. After the 10<sup>th</sup> application cycle, the treated mud briquettes samples were cured in a ventilated box for 28 days, under laboratory conditions ( $T = 20\text{-}25$  °C,  $\text{RH} = 60\text{-}80$  %).

At the end of the curing period, both treated and untreated specimens were placed in contact with water, in order to absorb water and evaluate the consolidation and stabilization efficacy of  $\text{Ca}(\text{OH})_2$  treatments.



Fig. 3 Laboratory synthesized clay briquettes, with different montmorillonite content and application procedure of the consolidation treatments

## 3. RESULTS

### 3.1. Chemical and Mineralogical Analysis of Mud-bricks

The mineralogical (Fig. 4; Table 4) and chemical (Table 5) examination of the archaeological mud-brick samples after chemical treatment indicated the presence of montmorillonite-Mt  $((\text{Na}, \text{Ca})_{0.33} (\text{Al}, \text{Mg})_2 (\text{Si}_4\text{O}_{10}) (\text{OH})_2 \cdot n\text{H}_2\text{O})$ , illite-I  $(\text{K}, \text{H}$

$_3\text{O}) (\text{Al}, \text{Mg}, \text{Fe})_2 (\text{Si}, \text{Al})_4 \text{O}_{10} [(\text{OH})_2 \cdot (\text{H}_2\text{O})]$ , kaolinite-kaol  $(\text{Al}_2\text{O}_3 \cdot 2\text{SiO}_2 \cdot 2\text{H}_2\text{O})$ , albite-ab  $(\text{Na}(\text{AlSi}_3\text{O}_8))$ , quartz-qtz  $(\text{SiO}_2)$  and calcite-cal  $(\text{CaCO}_3)$ .

As indicated in Table 4 and Table 5, montmorillonite, a clay mineral of the smectite group, was present in all samples, being responsible for the swelling phenomena observed in the mud-bricks.

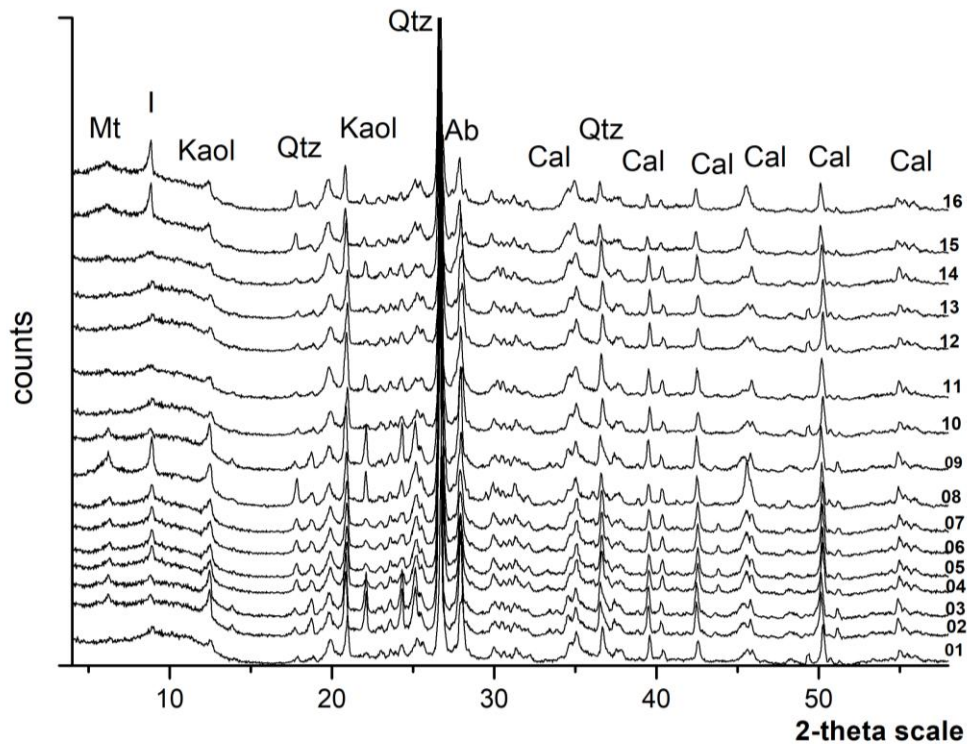


Fig. 4 X-ray diffraction patterns and semi-quantitative analysis of the sixteen mud-bricks

Table 3 Mineralogical analysis results of the sixteen mud-bricks, indicating the abundance of the main clay phases detected

	Quartz	Illite	Montmorillonite	Kaolinite	Albite
TB 12/01	++++	++++	+++	++	++
TB 12/02	++++	++++	++	++	++
TB 12/03	++++	+++	++	++	++
TB 12/04	++++	+++	+	++	+
TB 12/05	++++	+++	+	++	+
TB 12/06	++++	+++	++	++	+
TB 12/07	++++	++++	+++	++	++
TB 12/08	++++	++++	++	++	++
TB 12/09	++++	+++	++	++	++
TB 12/10	++++	++++	+++	+++	+++
TB 12/11	++++	++++	+++	+++	+++
TB 12/12	++++	++++	+++	+++	+++
TB 12/13	++++	++++	+++	+++	+++
TB 12/14	++++	+++	+	++	++
TB 12/15	++++	+++	+++	+++	++
TB 12/16	++++	++++	+++	++	+

**Table 4** Elemental analysis of the sixteen mud-bricks - split in two tables - expressed as percentage of the relevant oxides (% wt)

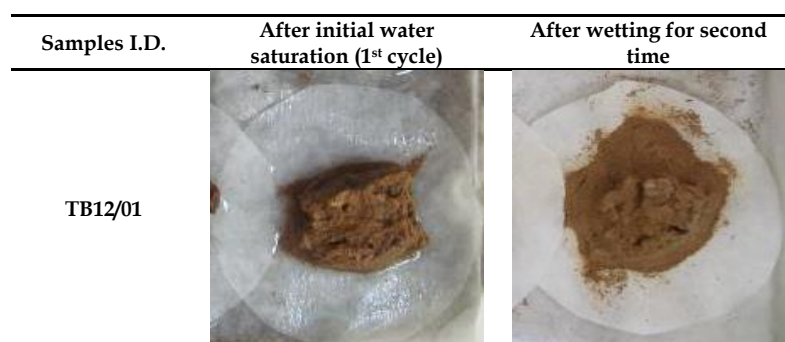
	TB12/01	TB12/02	TB12/03	TB12/04	TB12/05	TB12/06	TB12/07	TB12/08
Na <sub>2</sub> O	1.1	0.9	1.2	0.7	1	1.1	1.2	0.9
MgO	3.8	3.4	4.3	3.7	3.1	3.7	3.8	3.3
Al <sub>2</sub> O <sub>3</sub>	17.2	15.7	17.6	18	12.3	13.6	16.3	12.6
SiO <sub>2</sub>	52.6	55.4	54.7	55.4	58.6	52.6	52.7	42.9
P <sub>2</sub> O <sub>5</sub>	0.2	0.4	0.2	0.3	1.8	2.4	0	0.5
SO <sub>3</sub>	0.2	0.3	0.1	0	0.3	0	0	0
Cl <sub>2</sub> O	0.1	0.1	0.2	0	0.5	0.1	0	0
K <sub>2</sub> O	3.4	3.4	3.2	3.7	3.6	3.7	3.3	3.9
CaO	8.4	8.9	4.1	5.9	9.1	11.4	12.1	22.6
TiO <sub>2</sub>	1	1	1.1	1.1	0.9	0.9	0.7	0.9
Cr <sub>2</sub> O <sub>3</sub>	0.1	0.2	0.4	0.2	0.3	0.3	0.1	0.1
MnO	0.5	0.4	0.5	0.3	0.4	0.6	0.3	0.3
Fe <sub>2</sub> O <sub>3</sub>	9.8	8.9	11.4	9.7	7.2	8.1	8.9	10.8
NiO	0.4	0.3	0.5	0.3	0.4	0.3	0.2	0.2
CuO	0.7	0.3	0.3	0.4	0.2	0.5	0.2	0.5
ZnO	0.5	0.4	0.2	0.3	0.3	0.8	0.2	0.5
Total	1.1	0.9	100	100	100	100	100	100

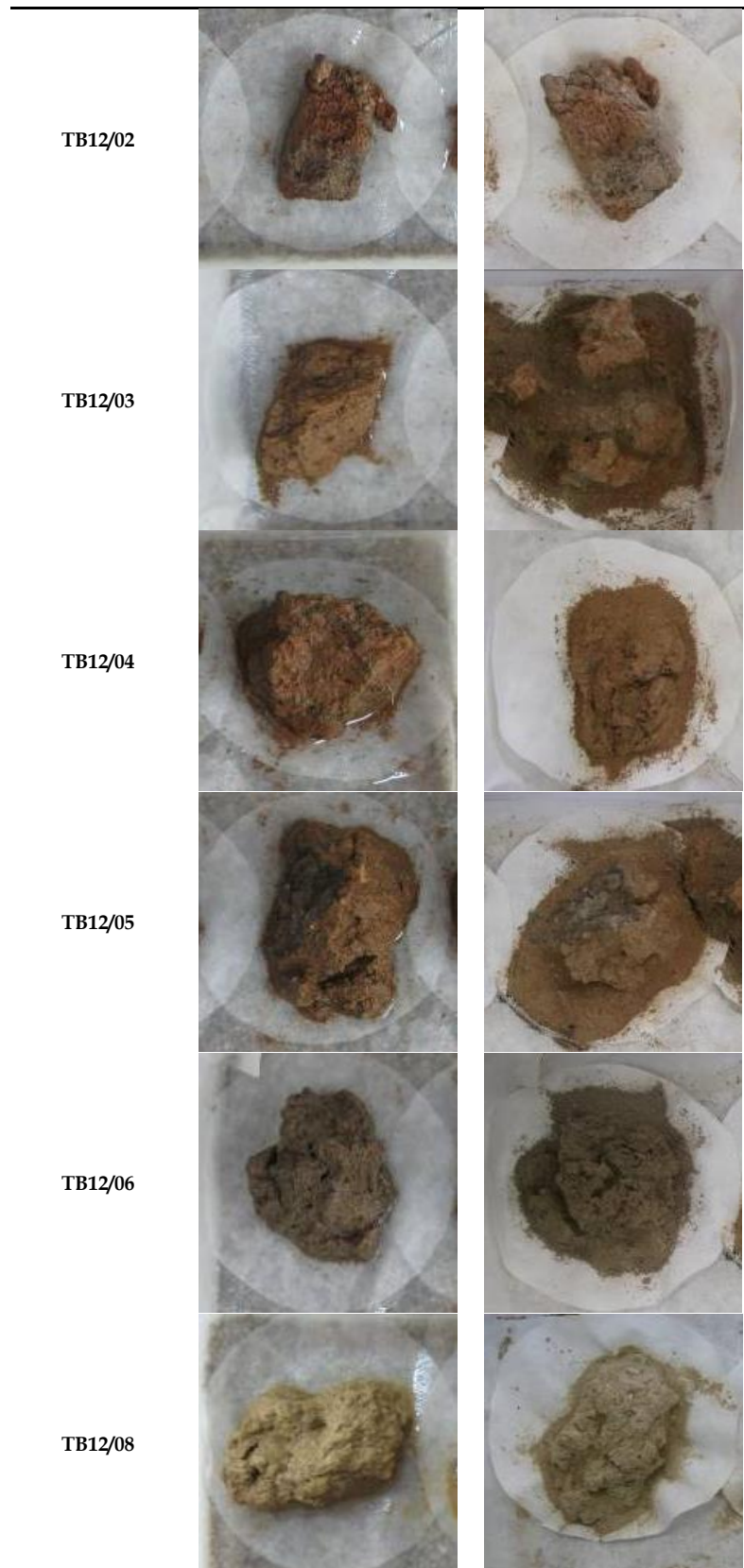
	TB12/09	TB12/10	TB12/11	TB12/12	TB12/13	TB12/14	TB12/15	TB12/16
Na <sub>2</sub> O	1.2	0.7	0.9	1.1	1.1	1	0.1	1.1
MgO	4.3	3.7	3.3	3.7	3.6	4.1	3.8	3.7
Al <sub>2</sub> O <sub>3</sub>	17.6	18	12.6	15.7	14.8	16.5	14.7	15.7
SiO <sub>2</sub>	54.7	55.4	42.9	56.9	52.7	53.2	53.6	56.9
P <sub>2</sub> O <sub>5</sub>	0.2	0.3	0.5	0.6	1.4	0.4	1.8	0.6
SO <sub>3</sub>	0.1	0	0	0.3	0.1	0.1	0.5	0.3
Cl <sub>2</sub> O	0.2	0	0	0.1	0.4	0.1	0.3	0.1
K <sub>2</sub> O	3.2	3.7	3.9	3.3	3.8	4.5	3.4	3.3
CaO	4.1	5.9	22.6	5.5	12.1	6.1	9.9	5.5
TiO <sub>2</sub>	1.1	1.1	0.9	1.1	0.9	1.2	1.1	1.1
Cr <sub>2</sub> O <sub>3</sub>	0.4	0.2	0.1	0.3	0.2	0.4	0.4	0.3
MnO	0.5	0.3	0.3	0.3	0.3	0.3	0.6	0.3
Fe <sub>2</sub> O <sub>3</sub>	11.4	9.7	10.8	10.4	8.2	10.7	8.2	10.4
NiO	0.5	0.3	0.2	0.2	0.1	0.5	0.6	0.2
CuO	0.3	0.4	0.5	0.3	0	0.4	0.4	0.3
ZnO	0.2	0.3	0.5	0.2	0.3	0.5	0.6	0.2
Total	100	100	100	100	100	100	100	100

### 3.2. Effect of water-drying cycles on the archaeological mud-bricks

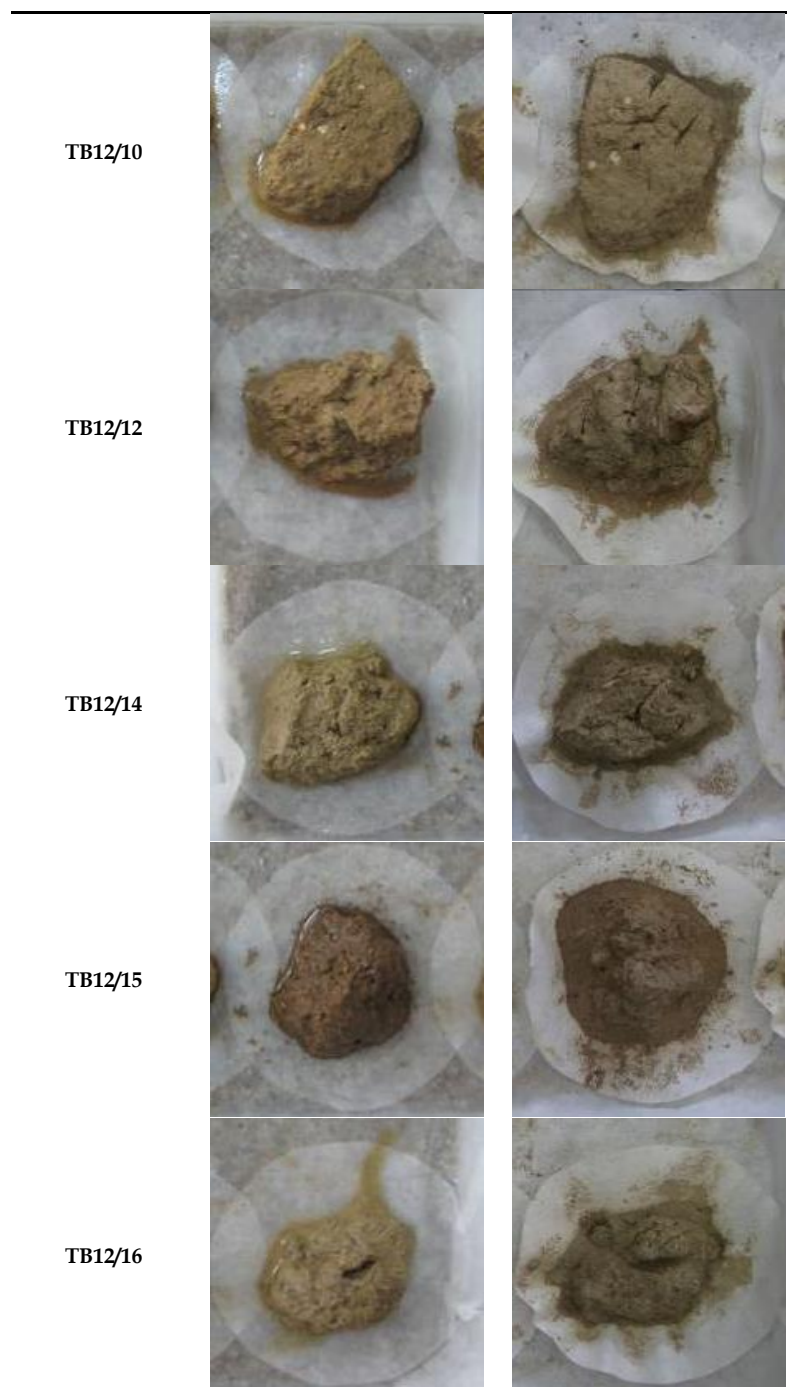
The evaluation of the response of the twelve selected archaeological mud-brick samples to the wet-drying cycles revealed the weathering effect of the swelling mechanism, leading to the collapse of the

samples after the drying process (Table 6). The collapse of the archaeological samples after the completion of the first wet-drying cycle was attributed to the presence of smectite minerals and specifically montmorillonite that was detected by XRD (Fig. 4; Table 4).

**Table 5** Macroscopic characterization of twelve mud-bricks subjected to 1 wet-drying cycle







### 3.3. Morphological characterization of laboratory prepared clay mixtures treated with $\text{Ca}(\text{OH})_2$

The morphological characterization of the reaction products resulted by the interaction between  $\text{Ca}(\text{OH})_2$  and the clay enriched with 1%wt of montmorillonite, was implemented by SEM at 24 hours and 1 month after their treatment. The microstructure presented in Fig. 5 is representative of the mor-

phology resulted in all three mixtures after 24 hours. In all samples large agglomerates with two distinct phases were detected, involving the presence of  $\text{Ca}(\text{OH})_2$  agglomerated nanoparticles and flake-like formations attributed to the clay phases. The chemical composition of each phase was determined by elemental analysis (EDAX), which is also included in Fig. 5.

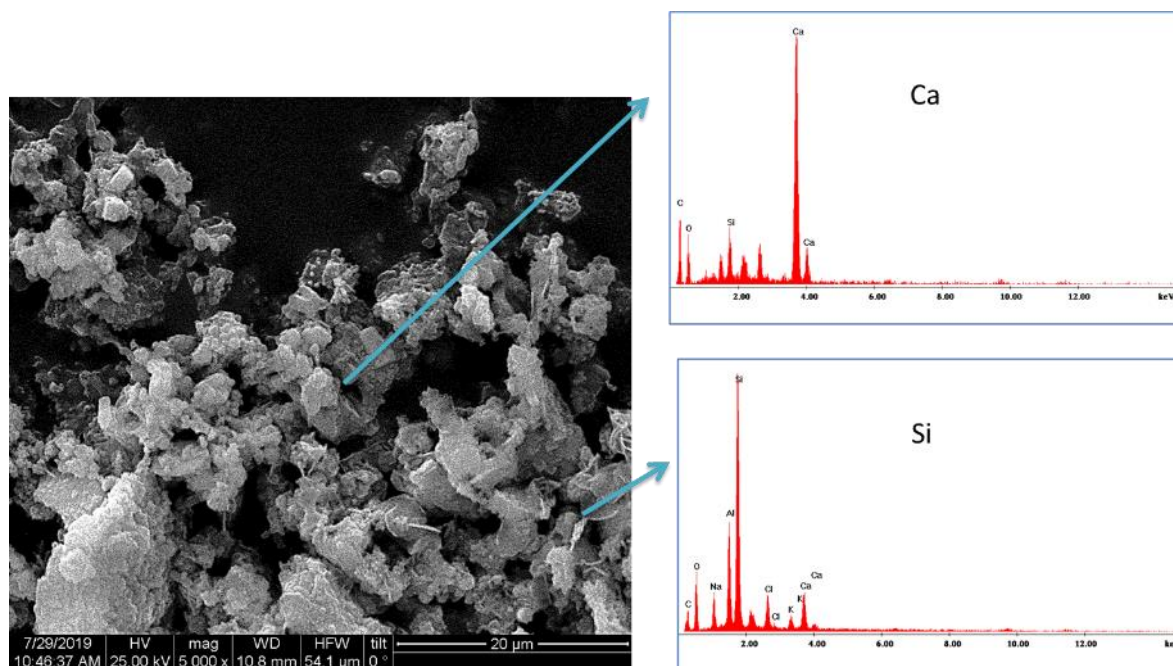


Figure 5 Representative SEM/EDAX photomicrograph, exhibiting the microstructure and the elemental analysis of the agglomerates detected after 24h, indicating the Ca-rich (Ca) and Si-rich (Si) phases

After 1 month, the micro-morphology of the three mixtures exhibited considerable differences (Fig. 6). The use of aqueous nanolime dispersion NW of plate-like homogeneous  $\text{Ca}(\text{OH})_2$  nanoparticles (Fig. 6a) resulted in the presence of more homogenous large agglomerates (Fig. 6b). Similarly, the use of hydro-alcoholic nanolime dispersion N/w+isp (Fig. 6c) resulted in the presence of large agglomerates of homogenous morphological characteristics (Fig. 6d). However, in the case of the clay mixture treated with aqueous  $\text{Ca}(\text{OH})_2$  saturated solution LW (Fig. 6e), the increased dimensions of the  $\text{Ca}(\text{OH})_2$  particles proved to affect the morphological characteristics of the initial clay mixture (Fig. 6f). Overall, the presence of large agglomerates along with the absence of a homogenous porous network was the morphological characteristic detected in all three mixtures.

### 3.4. Mineralogical characterization of laboratory prepared clay mixtures treated with $\text{Ca}(\text{OH})_2$

The mineralogical examination of laboratory clay mixtures with 1%wt montmorillonite content (Fig. 7) indicated the presence of montmorillonite-Mt ( $(\text{Na}, \text{Ca})_{0.33}(\text{Al}, \text{Mg})_2(\text{Si}_4\text{O}_{10})(\text{OH})_2 \cdot n\text{H}_2\text{O}$ ), kaolinite-kaol ( $\text{Al}_2\text{O}_3 \cdot 2\text{SiO}_2 \cdot 2\text{H}_2\text{O}$ ), illite-I ( $(\text{K}, \text{H}_3\text{O})(\text{Al}, \text{Mg}, \text{Fe})_2(\text{Si}, \text{Al})_4\text{O}_{10}[(\text{OH})_2 \cdot (\text{H}_2\text{O})]$ ), albite-ab ( $\text{Na}(\text{AlSi}_3\text{O}_8)$ ), quartz-qtz ( $\text{SiO}_2$ ) and calcite-cal ( $\text{CaCO}_3$ ).

The comparative evaluation of the mineralogical analysis of the three trials did not exhibit any differences. The elevated concentration of calcite ( $\text{CaCO}_3$ ) shadows the peaks corresponding to potential hydraulic (C-S-H or C-A-H) phases.



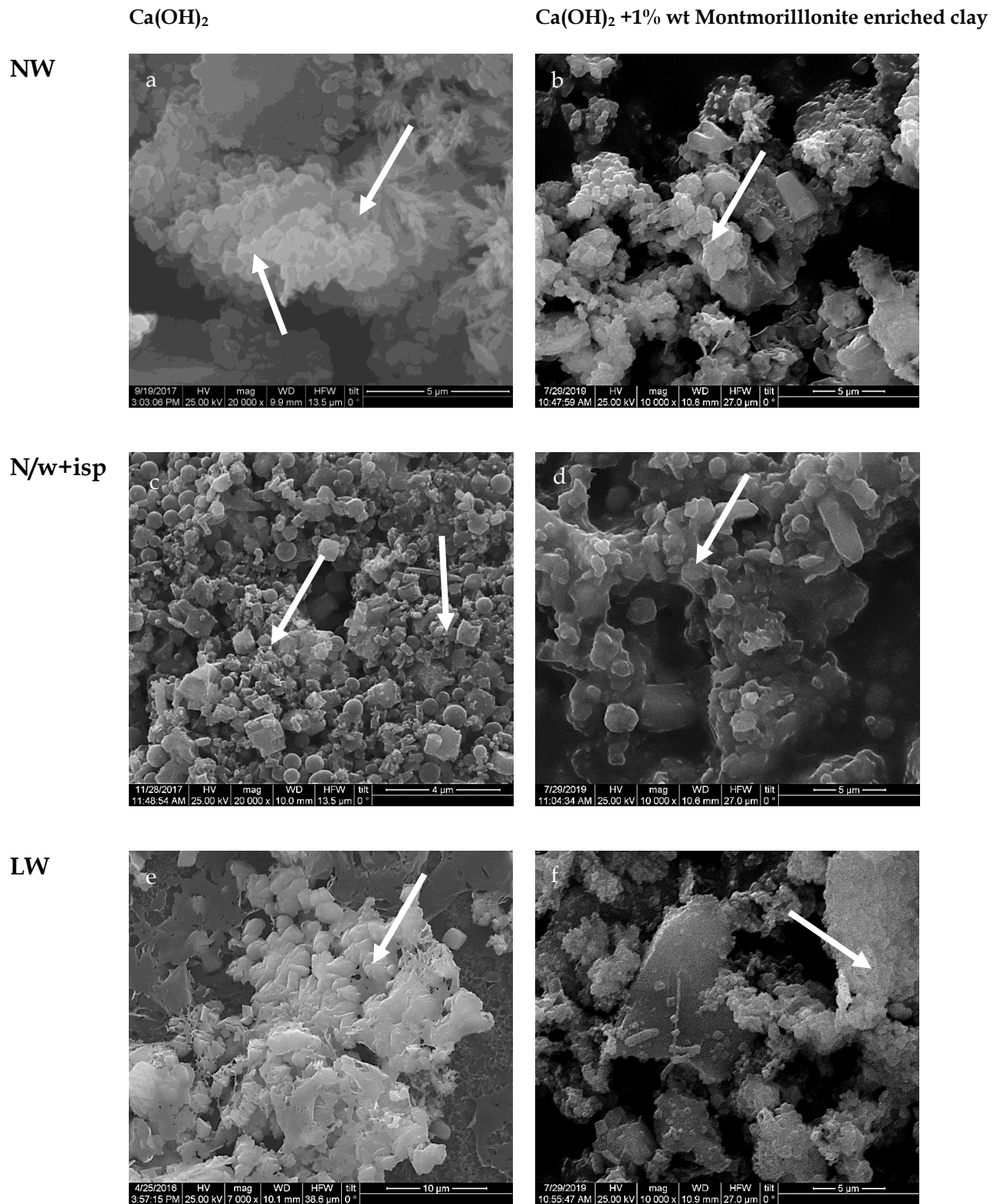


Fig. 6 Comparative evaluation between morphological characteristics of montmorillonite enriched clay (1% wt). treated with different forms of Ca(OH)<sub>2</sub>, after 1 month

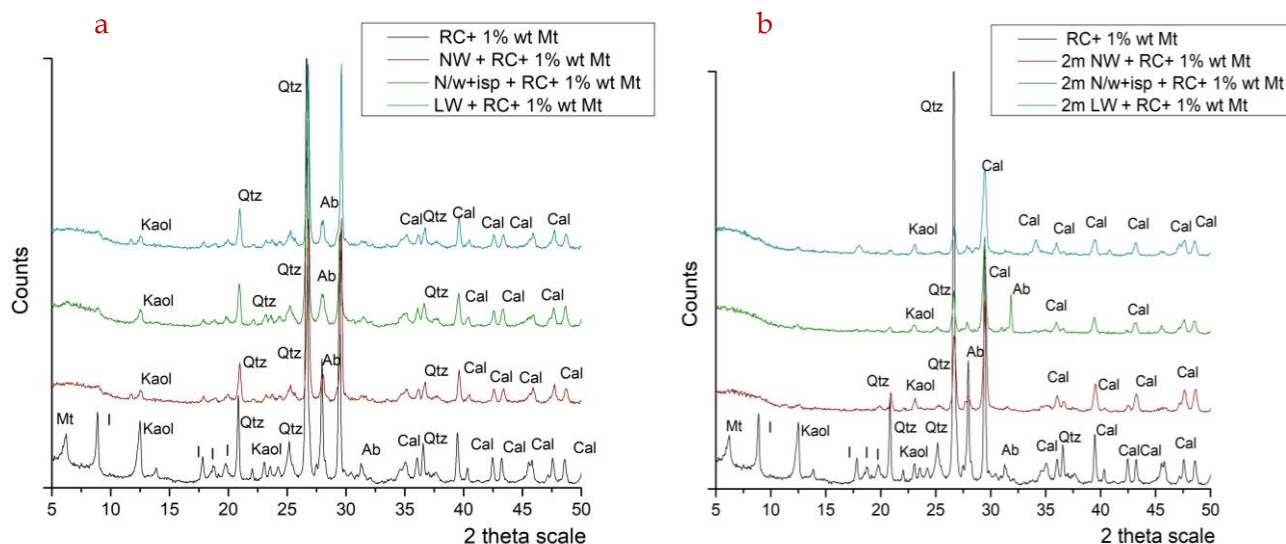


Fig. 7 X-ray diffraction patterns enriched clay mixtures enriched with montmorillonite (1% wt) after a) 24h and b) 2 months

### 3.5. Chemical characterization of laboratory prepared clay mixtures treated with $\text{Ca}(\text{OH})_2$

The FTIR analysis of the three treated clay mixtures after 24 hours presented similar results (Fig. 8). Specifically, the presence of the sharp band at  $3640\text{ cm}^{-1}$  corresponds to the OH- stretching modes of portlandite and the presence of humidity (Rodríguez-Navarro *et al.*, 2013). The presence of calcite was identified by the small and sharp band at  $1797\text{ cm}^{-1}$  corresponding to the C=O bonds of the carbonates  $-\text{CO}_3^{2-}$  (Galvan-Ruiz *et al.*, 2009), the broad band centred at  $1500\text{ cm}^{-1}$  corresponding to the  $\nu_2$  symmetric deformation of the carbonates  $-\text{CO}_3^{2-}$ , the  $870\text{ cm}^{-1}$  corresponding to the  $\nu_3$  asymmetric stretching of the carbonates  $-\text{CO}_3^{2-}$  and, finally the  $773\text{ cm}^{-1}$  corresponding to the  $\nu_4$  mode of the carbonates  $-\text{CO}_3^{2-}$ , underlying the carbonation of portlandite ( $\text{Ca}(\text{OH})_2$ ) to calcite ( $\text{CaCO}_3$ ) (Michalopoulou *et al.*, 2020; Rodríguez-Navarro *et al.*, 2013). The two bands at  $1121$  and  $1010\text{ cm}^{-1}$  were attributed to the Si-O  $\nu_3$  vibrations, while the smaller band at  $920\text{ cm}^{-1}$  was

attributed to the Si-O stretching vibrations (Barbenera-Fernandez *et al.*, 2015) (Fig. 8a, b and c). However, the FTIR analysis of the same samples after a time period of 2 months revealed the presence of C-S-H phases. Specifically, the interpretation of the spectra revealed a widening of the strong band at  $1176\text{ cm}^{-1}$  and  $1086\text{ cm}^{-1}$  corresponding to the Si-O  $\nu_3$  vibration, a shift of the band corresponding to the internal asymmetric Si-O-Si from  $1010$  to  $1041\text{ cm}^{-1}$  and the absence of the small and sharp band at  $920\text{ cm}^{-1}$  corresponding to the silanol group Si-O-Si (Barbenera-Fernandez *et al.*, 2015; Camerini *et al.*, 2018). According to the literature (Barbenera-Fernandez *et al.*, 2015), the gradual widening and unification of the  $1176$ ,  $1086$  and  $920\text{ cm}^{-1}$  corresponds to the presence of C-S-H phases, where the wider bands could be attributed to overlapping of the Ca-poor gels with the amorphous silica. The band around  $960\text{ cm}^{-1}$  could be attributed to the Si-O asymmetric stretching vibration of the C-S-H phases. This was more evident in the examination of the mixture containing the hydro-alcoholic nanolime dispersion N/w+isp (Fig. 8b).

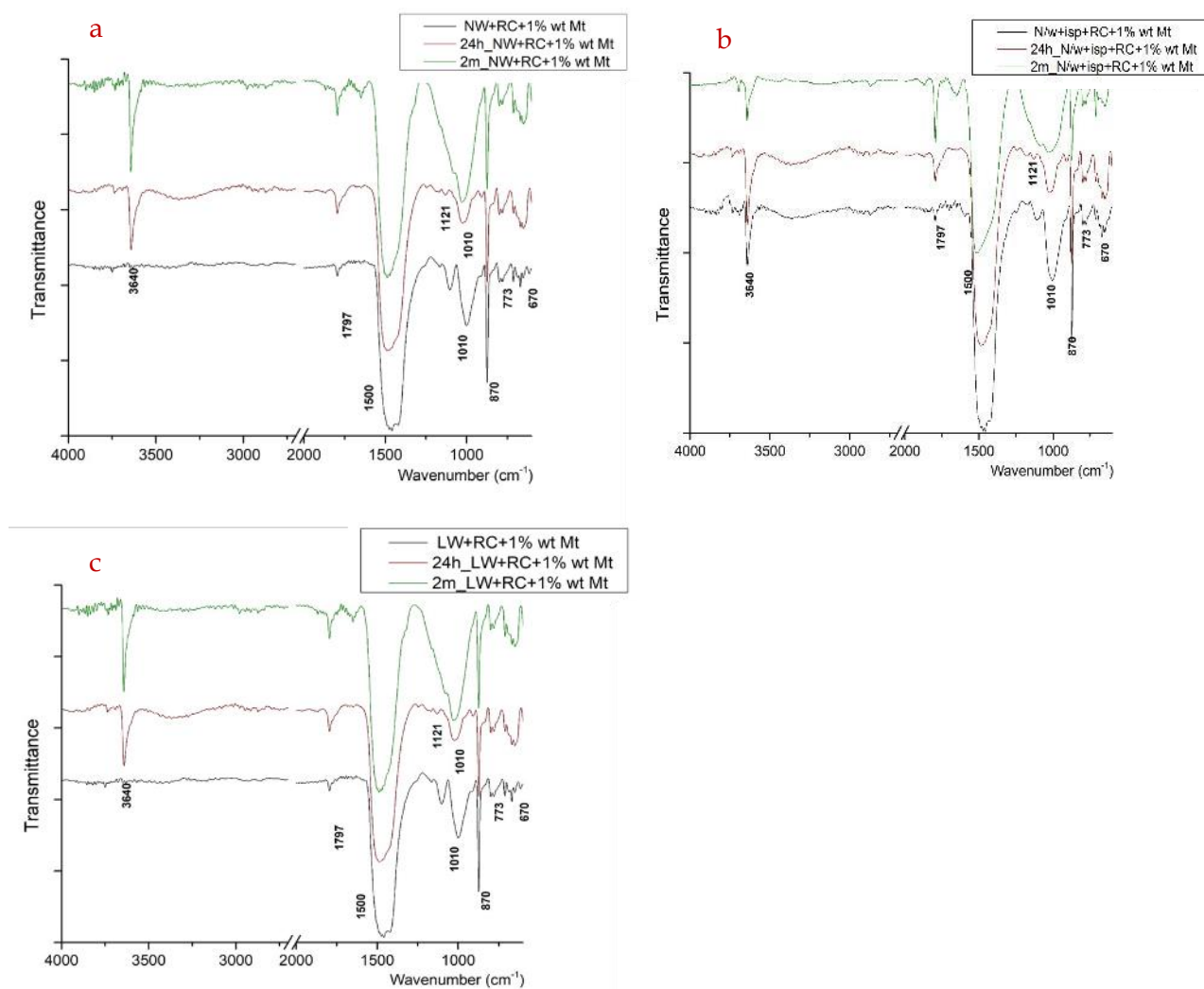


Fig. 8 FTIR spectra of montmorillonite enriched clay mixtures (1% wt), treated with different types of  $\text{Ca}(\text{OH})_2$ , at different curing periods

### 3.6. Stabilization Effectiveness of $\text{Ca}(\text{OH})_2$ treatments on the laboratory synthesized clay briquettes

A previously mentioned in section 3.5, the three  $\text{Ca}(\text{OH})_2$  treatments (NW, N/w+isp and LW) were applied drop to drop on the top face of the rectangular prismatic specimens with the use of a pipette for 10 consecutive applications. On every rectangular prismatic specimen, the red number indicated the corresponding percentage of montmorillonite (1, 5 and 15 % w/w) added during the preparation, along with a montmorillonite-free reference mixture indicated by the letter R. At the end of the application procedure, all briquettes appeared a whitening effect, attributed to the poor penetration of the  $\text{Ca}(\text{OH})_2$  treatments. This was more evident in the case of the application of the saturated aqueous solution LW, since the applied solution did not penetrate and instead, a film was formed on the surface of the briquettes due to the precipitation of  $\text{Ca}(\text{OH})_2$  particles.

It should be noted however that the density of the laboratory briquettes was much higher than that of the archaeological mud-bricks.

Upon the completion of the curing period, both treated and untreated briquettes were placed in contact with water, in order to assess the consolidation and stabilization efficacy of  $\text{Ca}(\text{OH})_2$  treatments. Upon wetting, all briquettes exhibited volume increase and material loss (Fig. 9). The untreated reference briquettes (Fig. 9, left column) presented severe degradation. The untreated briquettes that were enriched with montmorillonite presented more extensive degradation compared to the reference ones, without montmorillonite. The increase of montmorillonite content has resulted in the increased intensity of the swelling phenomenon, leading to the presence of large cracks and the eventual collapse of the briquettes (Fig. 9, framed final row).

Concerning the comparative evaluation of the three  $\text{Ca}(\text{OH})_2$  treatments, the application of the hy-

dro-alcoholic nanolime dispersion **N/w+isp** (Fig. 9, framed right column) seemed to reduce the swelling intensity and the degradation of the briquettes (Fig. 10). This was also evident in case of the aqueous nanolime dispersion **NW**, but at a lower degree (Fig.

9, 2nd column left). Finally, the application of the saturated aqueous solution **LW** did not affect the swelling capacity of the clay minerals (Fig. 9, 2nd column right), resulting a similar degradation effect with the untreated specimens.



Fig. 9 Degradation patterns of treated and untreated briquettes, subjected to water absorption

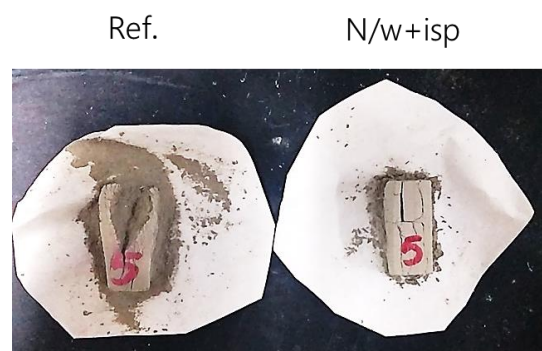


Fig. 10 Degradation patterns of laboratory prepared clay briquettes, enriched with montmorillonite (5 % wt).

#### 4. DISCUSSION

The elaboration of the results of the mineralogical and chemical characterization of the mud-bricks from the prehistoric settlement of Thessaloniki Toumba, as well as their response to repeated wet/drying cycles underlined the degradation effect of montmorillonite that leads to the gradual collapse of their microstructure. Specifically, during the preservation study of the mud-bricks obtained from the archaeological site, the correlation of the delete-

rious action of water along with the presence of montmorillonite clay mineral was established, leading to the presence of the swelling phenomenon and to the consequent collapse (Table 6).

The chemical characterization of the three treated clay-mixtures after a period of 2 months revealed the presence of the C-S-H phase (Fig. 8). According to the relevant literature (Elert *et al.*, 2015; Maskell *et al.*, 2014), the potential interactions between alkaline solutions and clay minerals might include: a) the implementation of the phenomenon of cation ex-



change between the cations in the interlayer of the clay minerals and the cation of the alkaline solution (Gaucher and Blanc, 2007), b) the encapsulation of the clay minerals, c) the absorption of organic molecules in the interlayer of the clay minerals (Tingle et al., 2003), d) the dissolution of the clay minerals and the transformation into pozzolanic (C-S-H) phases (Camerini et al., 2018; Elert et al., 2008; Karatasios et al., 2014) and e) the presence of flocculation phenomena resulted from the application of high concentrated alkaline solutions, promoting the reduction of both osmotic and intracrystalline swelling of clay minerals (Karnland et al., 2007). The interpretation of the chemical results revealed that the in-situ interaction between the  $\text{Ca}(\text{OH})_2$  and the montmorillonite (clay) mineral was based on the dissolution of the alumino-silicates, the reaction between the  $\text{Ca}^{2+}$  and the  $\text{SiO}_2$  and the formation of new C-S-H phase (Fig. 8). This has been reported during the mineralogical examination of the ancient roman mortars. The enhanced durability of the ancient roman mortars was attributed to the presence of the new C-S-H phase (Elert et al., 2015; Roy, 1999). The lack of detection of C-S-H phases in the XRD results (Fig. 7), along with the absence a homogeneous porous network of crumpled foils (Camerini et al., 2018) in the morphological characterization of the mixtures (Fig. 6) underlined the need of a longer period for the completion of the synthesis of the C-S-H phase.

The preliminary evaluation of the consolidation efficacy of the two nanolime dispersions (**NW** and **N/w+isp**) applied on laboratory prepared briquettes verified the in-situ interaction between the  $\text{Ca}(\text{OH})_2$  nanoparticles and montmorillonite. Only the treated briquettes enriched with 1% wt and 5% wt of montmorillonite presented a reduction of the swelling phenomenon (Fig. 9 and 10), causing the reduction of volume changes and increasing the durability of mud- briquettes against water. The reduction of swelling capacity of montmorillonite was more evident in the case of hydro-alcoholic nanolime dispersion **N/w+isp** (Fig. 9 and 10). This was attributed to three factors: a) the partial replacement of water with 2-propanol, leading to the reduction of the presence of water, which has been connected with the swelling phenomenon, in respect with the aqueous nanolime dispersion (**NW**), b) the reduced size along with the increase content of the  $\text{Ca}(\text{OH})_2$  nanoparticles, in respect with the aqueous saturated solution (**LW**) and c) the use of 2-propanol that promotes the increase of the penetration ability of the nanolime dispersions. The final reduction of the swelling capacity of monmortillonite enriched briquettes after their treatment with nanolime ( $\text{Ca}(\text{OH})_2$ ) dispersions, in-

dicated the potential of both hydro-alcoholic and aqueous nanolime dispersions as an effective alternative to traditional preservation and consolidation treatments (Elert et al., 2015; Lanzon et al., 2020; Stefanis et al., 2010). Finally, the appearance of the whitening effect was attributed to the poor penetration of  $\text{Ca}(\text{OH})_2$  treatments, due to the compact microstructural and pore network characteristics of the clay briquettes (Michalopoulou et al., 2020; Otero et al., 2018).

Overall, the study of different  $\text{Ca}(\text{OH})_2$  dispersions as potential swelling inhibitors provided promising results that highlight their potential in the consolidation and stabilization of archaeological mud-bricks, both in laboratory and in-situ application.

## 5. CONCLUSIONS

The preservation study of the mud-bricks collected during the excavation of the prehistoric settlement of Thessaloniki Toumba revealed the correlation between the deleterious act of water along with the presence of montmorillonite clay mineral (smectite group), characterized by the appearance of the swelling phenomenon that leads to the eventual material collapse.

The comparative evaluation of three  $\text{Ca}(\text{OH})_2$  treatments belonging in two different categories: saturated solution of calcium hydroxide and different types of laboratory synthesized nanophase lime dispersions, revealed their potential as swelling inhibitors.

- The interaction between  $\text{Ca}(\text{OH})_2$  and the alumino-silicate clay minerals revealed the formation of new C-S-H phases.
- The use of hydro-alcoholic dispersion medium promoted the anti-swelling capacity of the  $\text{Ca}(\text{OH})_2$  treatments, through the reduction of water.
- The reduced size, increased specific surface area and increased content of the  $\text{Ca}(\text{OH})_2$  nanoparticles proved to promote the interaction between  $\text{Ca}(\text{OH})_2$  and clay minerals.

$\text{Ca}(\text{OH})_2$  nano-dispersions were more effective on the stabilization of montmorillonite enriched clay briquettes when subjected to the water absorption test. However, an optimum balance between water and 2-propanol should be considered at each case of application, in order to provide the necessary amount of water for the formation of C-S-H phases and at the same time diminish the contribution of water to the swelling phenomenon.

## ACKNOWLEDGMENTS

We acknowledge the support of this work by the project "Development of Materials and Devices for Industrial, Health, Environmental and Cultural Applications" (MIS 5002567) which is implemented under the "Action for the Strategic Development on the Research and Technological Sector", funded by the Operational Programme "Competitiveness, Entrepreneurship and Innovation" (NSRF 2014-2020) and co-financed by Greece and the European Union (European Regional Development Fund).

## REFERENCES

- Abd-Allah, R., Al-Muheisen, Z. and Al-Howadi, S. (2010) Cleaning strategies of pottery objects excavated from Khirbet Edh-Dharrah and Hayyan al-Mushref, Jordan: four case studies. *Mediterranean Archaeology and Archaeometry*. Vol. 10. No. 2. pp. 97-110.
- Andreou, S. (2007) Stratified Wheel made Pottery Deposits and Absolute Chronology at Thessaloniki Toumba and the EIA-LBA Transition in Thessaloniki Toumba. In Deger-Jalkotzy, S. and A. Bächle (eds). LH III C Late and the Transition to the Early Iron Age. International Workshop held at the Austrian Academy of Sciences at Vienna, February 23rd and 24th 2007 15-40. Wien: Verlag der Österreichischen Akademie der Wissenschaften.
- Andreou, S., Fotiadis, M. and Kotsakis, K. (1996) Review of Aegean Prehistory V: The Prehistoric and Bronze Age of Northern Greece. *American Journal of Archaeology*. Vol. 100. pp. 537-597.
- Barbenera-Fernandez, A.M., Carmona-Qioroga, P.M. and Blanco-Varela, M.T. (2015) Interaction of TEOS with cementitious materials: Chemical and physical effects. *Cement and Concrete Composites*. Vol. 55. pp. 145-152.
- Borsoi, G., Lubelli, B., VanHees, R., Veiga, R., Santos Silva, A., Colla, L., Fedele, L. and Tomasin, P. (2016) Effect of solvent on nanolime transport within limestone: How to improve in-dept deposition. *Colloids and Surfaces A: Physicochemical and Engineering Aspects*. Vol. 497. pp. 171-181.
- Camerini, R., Chelazzi, D., Giorgi, R. and Baglioni, P. (2018) Hybrid nano-composites for the consolidation of earthen masonry. *Journal of Colloid and Interface Science*. Vol. 539. pp. 504-515.
- Chen, W., Zhang, Y., Zhang, J. and Dai, P. (2018) Consolidation effect of composite materials on earthen sites. *Construction and Building Materials*. Vol. 187. pp. 730-737.
- Crosby, A. (1988) The causes and effects of decay on adobe structures. In the *5th International Meeting of Experts on the Conservation of Earthen Architecture*. 22-23 October 1987. Rome. Italy
- Daniele, V. and Taglieri, G. (2012) Synthesis of Ca(OH)<sub>2</sub> Nanoparticles with the Addition of Triton X-100. Protective Treatments on Natural Stones: Preliminary Results. *Journal of Cultural Heritage*. Vol. 13. No. 1. pp. 40-46.
- Daniele, V., Taglieri, G. and Gregori, A. (2013) Synthesis of Ca(OH)<sub>2</sub> nanoparticles aqueous suspensions and interaction with silica fume. *Advanced Materials Research*. Vol. 629. pp. 482-487.
- El-Derby, A. and Elyamani, A. (2016) The adobe barrel vaulted structures in ancient Egypt: A study of two case studies for conservation purposes. *Mediterranean Archaeology and Archaeometry*. Vol. 16. No. 1. pp. 295-315.
- El-Gohary, M. and Al-Naddaf, M.M. (2009) Characterization of bricks used in the external casing of roman bath walls. *Mediterranean Archaeology and Archaeometry*. Vol. 9. No. 2. pp. 29-46.
- Elert, K., Pardo, E.S. and Rodriguez-Navarro, C. (2015) Alkaline activation as an alternative method for the consolidation of earthen architecture. *Journal of Cultural Heritage*. Vol. 16. pp. 461-469.
- Elert, K., Sebastian, E., Valverde, I. and Rodriguez-Navarro, C. (2008) Alkaline treatment of clay minerals from the Al-hambra Formation: implications for the conservation of earthen architecture. *Construction and Building Materials*. Vol. 39. pp. 122-132.
- Emiroğlu, M., Yalama A. and Abdekmadjid, H. (2015) Performance of ready-mixed clay plasters produced with different clay/sand ratios. *Applied Clay Science*. Vol. 115 pp. 221-229.
- Galvan-Ruiz, M., Hernandez, J., Banos, L., Noriega-Montes, J. and Rodriguez-Garcia, M.E. (2009) Characterization of calcium carbonate, calcium oxide, and calcium hydroxide as Starting Point to the Improvement of Lime for Their Use in Construction. *Journal of Materials of Civil Engineering*. Vol. 21. No. 11. pp. 694-696.
- Garcia-Vera, V. and Lanzon, M. (2018) Physical-chemical study, characterisation and use of image analysis to assess the durability of earthen plasters exposed to rain water and acid rain. *Construction and Building Materials*. Vol. 187 pp. 708-717.



- Garcia-Vera, V.E., Tenza-Abril, J., Solak, A.M. and Lanzón, M. (2020) Calcium hydroxide nanoparticles coatings applied on cultural heritage materials: Their influence on physical characteristics of earthen plasters. *Applied Surface Science*. Vol. 504. 144195.
- Gaucher, E.C. and Blanc, P. (2007) Cement/clay interactions-a review: experiments. natural analogues. and modeling.. *Waste Management*. Vol. 36. No. 7 pp. 776-788.
- Hall, M. and Djerbib, Y. (2004) Rammed earth sample production: Context. recommendations and consistency. *Construction and Building Materials*. Vol. 18. No. 4. pp. 281-286.
- Hensen, E.J.M. and Smit, M. (2002) Why clays swell. *Journal of Physical Chemistry B*. Vol. 106. pp. 12664-12667.
- Jimenez-Delgado, M.C. and Guerrero, I.C. (2006) Earth building in Spain. *Construction and Building Materials*. Vol. 20. pp. 679-690.
- Karatasios, I., Alexiou, K., Muller, N.S., Day, P.M. and Kilikoglou, V. (2014) The second life of ceramics: a new home in a lime environment. In: *Craft and science: International perspectives on archaeological ceramics*. Bloomsbury Qatar Foundation. Doha. Qatar
- Karatasios, I., Theoulakis, P., Kalagri, A., Sapalidis, A. and Kilikoglou, V. (2009) Evaluation of consolidation treatments of marly limestones used in archaeological monuments. *Construction and Building Materials*. Vol. 23. pp. 2803-2812.
- Karnland, O., Olsson, S., Nilsson, U. and Sellin, P. (2007) Experimental determined swelling pressures and geochemical interactions of compacted Wyoming bentonite with highly alkaline solutions. *Physics and Chemistry of the Earth. Parts A/B/C*. Vol. 32. pp. 275-286.
- Lanzon, M., De Stefano, V., Molina Gaitán, J.C., Bestué Cardiel, I. and Lourdes Gutiérrez-Carrillo, M.L. (2020) Characterisation of earthen walls in the Generalife (Alhambra): Microstructural and physical changes induced by deposition of  $\text{Ca}(\text{OH})_2$  nanoparticles in original and reconstructed samples. *Construction and Buildings Materials*. Vol. 232. 117202.
- Lanzon, M., Madrid, J.A., Martínez-Arredondo, A. and Monaco, S. (2017) Use of diluted  $\text{Ca}(\text{OH})_2$  suspensions and their transformation into nanostructured  $\text{CaCO}_3$  coatings: A case study in strengthening heritage materials (stucco, adobe and stone). *Applied Surface Science*. Vol. 424. No.1. pp. 20-28.
- Lawrence, M., Heath, A., Fourie, P. and Walker, P. (2009) Compressive strength of extruded unfired clay masonry units. *Construction Materials and Structures*. Vol. 162. No. 3. pp. 105-112.
- Lorenzon, M., Nitschke, J.L., Littman, R.J. and Silverstein, J.E. (2020) Mudbricks. Construction Methods. and Stratigraphic Analysis: A Case Study at Tell Timai (Ancient Thmuis) in the Egyptian Delta. *American Journal of Archaeology*. Vol. 124. No. 1. pp. 105-131.
- Love, S. (2012) The Geoarchaeology of Mudbricks in Architecture: A Methodological Study from Çatalhöyük. Turkey. *Geoarchaeology*. Vol. 27. No. 2. pp. 140-156.
- Maravelaki-Kalaitzaki, P., Kallithrakas-Kontos, N., Agioutantis, Z., Maurigiannakis, S. and Korakaki, S. (2008) A comparative study of porous limestones treated with silicon-based strengthening agents. *Progress in Organic Coatings*. Vol. 62. No. 1. pp. 49-60.
- Maskell, D., Heath, A. and Walker, P. (2014). Inorganic stabilisation methods for extruded earth masonry units. *Construction and Buildings Materials*. Vol. 71. pp. 602-609.
- Medjo Eko, R., Dieudonné Offa, E., Yatchoupou Ngatcha, T. and Seba Minsili, L. (2012) Potential of salvaged steel fibers for reinforcement of unfired earth blocks. *Construction and Building Materials*. Vol. 35. pp. 340-346.
- Michalopoulou, A., Favvas, E.P., Mitropoulos, A.C., Maravelaki, P., Kilikoglou, V. and Karatasios, I. (2018). A comparative evaluation of bottom-up and top-down methodologies for the synthesis of calcium hydroxide nanoparticles for the consolidation of architectural monuments. *Materials Today: Proceedings*. Vol. 5. No. 14. pp. 27425-27433.
- Michalopoulou, A., Michailidi, E., Favvas, E., Maravelaki, N.P., Kilikoglou, V. and Karatasios, I. (2020) Comparative evaluation of the morphological characteristics of nanolime dispersions for the consolidation of architectural monuments. *International Journal of Architectural Heritage*. Vol. 14. No.7. pp. 994-1007.
- Minke, G. (2012) *Building with Earth Design and Technology of a Sustainable Architecture*. Basel. Birkhäuser.
- Pham, H. and Nguyen, Q.M. (2014) Effect of silica nanoparticles on clay swelling and aqueous stability of nanoparticle dispersions. *Journal of Nanoparticle Research*. Vol. 16. No. 2137.
- Otero, J., Starinieri, V. and Charola, A.E. (2018) Nanolime for the consolidation of lime mortars: A comparison of three available products. *Construction and Building Materials*. Vol. 181. pp. 394-407.

- Otero, J., Starinieri, V., Charola, A.E. and Taglieri, G. (2020) Influence of different types of solvent on the effectiveness of nanolime treatments on highly porous mortar substrates. *Construction and Building Materials*. Vol. 232. 117112.
- Quagliarini, E. and Lenci, S. (2010) The influence of natural stabilizers and natural fibres on the mechanical properties of ancient Roman adobe bricks. *Journal of Cultural Heritage*. Vol. 11. pp. 309–314.
- Quagliarini, E., D' Orazio, M. and Lenci, S. (2015) The properties and durability of adobe earth-based masonry blocks In *Eco-Efficient Masonry Bricks and Blocks Design. Properties and Durability*. pp. 361–378. Cambridge. Elsevier.
- Ouhandi, V.R., Yong, R.N., Amiri, M. and Ouhandi, M.H. (2014) Pozzolanic consolidation of stabilized soft clays. *Applied Clay Science*. Vol. 95. pp. 111–118.
- Rainer, L. (2008) Deterioration and Pathology of Earthen Architecture in *Terra Literature Review: An Overview of Research in Earthen Architecture Conservation*. The Getty Conservation Institute. Los Angeles. USA.
- Rodriguez-Navarro, C., Suzuki, A. and Ruiz-Agudo, E. (2013) Alcohol Dispersions of Calcium Hydroxide Nanoparticles for Stone Conservation. *Langmuir*. Vol. 29. No. 36. pp. 11457–11470.
- Roy, D.N. (1999) Alkali-activated cements: Opportunities and challenges. *Cement and Concrete Research*. Vol. 29. pp. 249–254.
- Sáenz-Martínez, A., San Andrés, M., Alvarez de Buergo, M., Blasco, I. and Fort R. (2019) Removing calcium carbonate deposits from archaeological ceramics. traditional methods under review. *Mediterranean Archaeology and Archaeometry*, Vol. 19. No 3. pp. 107–117.
- Salama, K.K., Ali, M.F. and El Sheikh, S.M. (2019) Comparison between nano calcium carbonate, natural calcium carbonate and converted calcium hydroxide for consolidation. *Scientific Culture*. Vol. 5. No. 3. pp. 35–40.
- Salles, F., Douillard, J.M., Bildstein, O., Gaudin, C., Prelot, B., Zajac, J. and Van Dammec, H. (2013) Driving force for the hydration of the swelling clays: Case of montmorillonites saturated with alkaline-earth cations *Journal of Colloid and Interface Science*. Vol. 395. pp. 269–276.
- Seco, A., Ramirez, F., Miqueleiz, L. and Garcia, B. (2011) Stabilization of expansive soils for use in construction. *Applied Clay Science*. Vol. 51. pp. 348–352.
- Stefanis, N.A., Chatzi, K., Zioga, K. and Theoulakis, P. (2010). Study for the in situ preservation of the clay architectural elements from the excavation of the Prehistoric settlement of Dispilio. Greece. In: *8th International Symposium on the Conservation of Monuments in the Mediterranean Basin: Monument Damage Hazards and Rehabilitation Technologies*. 31 May – 2 June 2010. Patras. Greece
- Tingle, J. and Santoni, R. (2003) Stabilization of clay soils with non-traditional additives. *Transportation Research Record Journal of the Transportation Research Board*. Vol. 1819. No. 1 pp. 72–84.
- Xanthopoulou, V., Iliopoulou, I., and Liritzis, I. (2020) Characterization techniques of clays for the archaeometric study of ancient ceramics: a review. *Scientific Culture*. Vol. 6. No. 2. pp. 73–86.
- Wangler, T. and Scherer, G.W. (2008) Clay swelling mechanism in clay-bearing sandstones. *Environmental Geology*. Vol. 56. pp. 529–534.
- Zarzuela, R., Luna, M., Carrascosa, L.M., Yeste, M.P., Garcia-Lodeiro, I., Blanco-Varela, M.T., Cauqui. Rodriguez-Izquierdo, J.M. and Mosquera, M.J. (2020) Producing C-S-H gel by reaction between silica oligomers and portlandite: A promising approach to repair cementitious materials. *Cement and Concrete Research*. Vol. 130 pp. 776–788.